The Impact of Head Movements on EEG and Contact Impedance: An Adaptive Filtering Solution for Motion Artifact Reduction

Vojkan Mihajlović[1], Shrishail Patki[1], Bernard Grundlehner[1]

Abstract— **Designing and developing a comfortable and convenient EEG system for daily usage that can provide reliable and robust EEG signal, encompasses a number of challenges. Among them, the most ambitious is the reduction of artifacts due to body movements. This paper studies the effect of head movement artifacts on the EEG signal and on the dry electrode-tissue impedance (ETI), monitored continuously using the imec's wireless EEG headset. We have shown that motion artifacts have huge impact on the EEG spectral content in the frequency range lower than 20Hz. Coherence and spectral analysis revealed that ETI is not capable of describing disturbances at very low frequencies (below 2Hz). Therefore, we devised a motion artifact reduction (MAR) method that uses a combination of a band-pass filtering and multi-channel adaptive filtering (AF), suitable for real-time MAR. This method was capable of substantially reducing artifacts produced by head movements.**

I. INTRODUCTION

Recent technological developments in the area of noninvasive monitoring of electrical activity of the brain (electroencephalography, EEG) focus on sensors that do not use conductive gel and skin preparation. Instead, so called dry-contact electrodes, as well as more convenient headsets, are used [1]. Although such solutions offer advantages by enabling short setup time, higher comfort and convenience for the user, and the use by non-expert users in a daily life situation, they also come with drawbacks. Ensuring high signal quality in uncontrolled environment of daily life recordings becomes extremely difficult, as the contact between the electrode and the skin is much more fragile and prone to various type of noise and interference. These problems are emphasized during movement as motion artifacts result in substantial distortion of the recorded signal, such that EEG can hardly be recognized. In this paper we study the motion artifacts produced during head movements, and we present an approach to reduce the impact of such movement artifacts on the EEG signal.

A. Motion artifacts

Motion artifacts in EEG recordings are electrical disturbances of the measured EEG signal due to motion. They share the same frequency spectra with EEG (up to 50Hz) and they can have amplitudes several times larger than the EEG signal (in the order of a few mV). Due to the non-stationary nature and spectral overlap of EEG signal and artifacts, handling motion artifacts is challenging task that requires tailored EEG system design and development [2], [3]. Such task becomes even more difficult when dry electrodes are used, as they have different electrode-skin contact properties than gel-based electrodes [4]. User motion results in changes of the geometry of the contact between the electrodes and the skin and hence changes in the electrical coupling between the two. Furthermore, charge redistribution at the contact due to skin and tissue deformation takes place.

B. State-of-the-art in motion artifacts handling

In most EEG studies users are instructed not to move. In the analysis, segments with motion artifacts are excluded if they occur in the signal. Only a handful of papers discusses MAR approaches for (gel-based) EEG monitoring applications. They usually focus only on either detecting motion artifacts [5], [6], or reducing artifacts when regular movements are performed, such as human locomotion [2] or electrode movement (e.g., pushing or pulling) [7], [8]. The approaches by O'Regan et al. [5], [6] were focused on using gyroscopes and machine learning techniques in classifying recorded signal into segments contaminated with motion artifacts and clean segments. Achieved detection accuracy was high, but detecting motion artifacts is just a first step in MAR. Although substantial reduction of motion artifacts was achieved in [2], the complex setup used for artifact handling, that includes video monitoring, cannot easily be translated to a lifestyle setting. The approaches by Sweeney et al. [7], [8] were focused on using the differential signal from accelerometers to characterize the impact of electrode motion relative to the skin. The usage of these signals showed good performance on classifying artifacts according to their severity but showed limited usefulness when advanced algorithms are employed for MAR [8]. This suggests that accelerometer information has limited usefulness and can only capture some aspect of the motion artifact.

C. Handling motion artifacts using ETI

Relative movement of the electrode on the scalp and deformation of the skin underneath induce changes in the electrical properties of the contact interface. We argue that the absolute value of the electrode-tissue impedance (ETI) magnitude does not impact the signal quality of the measured EEG [9], but the relative changes that are occurring at the interface do. In our previous study we have observed that the ETI changes correlate with the changes happening at the dry electrode-skin contact interface during motion artifacts [10]. We have also explored the usage of ETI for off-line motion artifact reduction (MAR) [11]. By using canonical correlation

[1]V. Mihajlović, S. Patki, and B. Grundlehner are with Holst Centre / imec The Netherlands, 5656AE Eindhoven, The Netherlands {vojkan.mihajlovic, shrishail.patki, bernard.grundlehner} at imec-nl.nl

978-1-4244-7929-0/14/$26.00 ©2014 IEEE

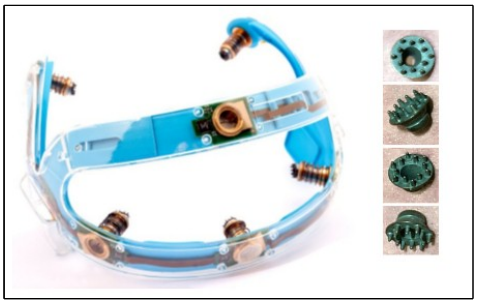

Fig. 1. The evaluation setup: imec's EEG headset and dry electrodes.

analysis and multi-channel linear prediction methods we have shown that combining ETI components (magnitude, in-phase, and quadrature), not only from a single but also from multiple channels, helps in reducing motion artifacts. In this paper we explore further what is the impact of head movements on the EEG and ETI, and we propose a method that combines band-pass filtering (BPF) and adaptive filtering (AF) approach for real-time MAR. We also investigated the degree in which motion artifacts can be suppressed by varying the number of ETI components in the AF algorithm.

II. METHODS

A. Experimental setup and recoding protocol

The experiment was performed using the wireless imec EEG headset, shown in Figure 1. It has the capability of continuously measuring EEG and ETI signal at 1024Hz [12]. Commercially available dry Ag/AgCl electrodes with pins are used to penetrate the hair and they are mounted on a spring-loaded support to ensure good contact with the skin, and more comfort to a user (see Figure 1). Active electrode chips that buffer the electrical signal are placed directly on top of the spring-loaded contact to prevent noise from entering the system as much as possible. In addition, they inject a small current (up to 200nA) to perform ETI measurement. The headset measures the potential difference between measurement electrodes at locations C3, C4, Cz, and Pz, of the International 10-20 System for EEG measurements, and the reference electrode positioned at the right earlobe.

The database consisted of the recordings obtained on six participants, performing different types of movement as explained in our previous work [11]. For this study we focused only on the head movements, while participants had their eyes either open or closed:

- *Head nodding*: The experiment started with 60s period where the participant was sitting straight and no head movements were involved. The participant was then asked to nod his head for 60s. The session was finished with 60s period with no movements involved.
- *Head shaking*: The experiment started with 60s where the participant was sitting and no head movements were involved. The participant was then asked to shake his head for 60s. The session finished with period of 60s with no movements involved.

B. EEG and impedance signal analysis

EEG and impedance signals were preprocessed by applying different filters. A stop-band filter (third order Butterworth filter) in the frequency range of 49 to 51Hz was used to eliminate power line noise. ETI signals were filtered with a high-pass, first order, Butterworth filter at 0.194Hz, since a similar filter is applied to the EEG signals by the hardware solution [12]. After preprocessing, we investigated the spectral properties of filtered EEG and impedance signals by comparing spectral coherence and power spectral densities in presence and in absence of motion artifacts. Spectral properties are estimated using the well-known Welch method. Epochs with a 2s duration and 75% of overlap were used in the analysis.

C. Adaptive filter based approach for MAR

The MAR approach consists of two steps. In the first step, band-pass filter (BPF) is applied to the EEG and impedance signal. We used a third order Butterworth filter. Suitable cutoff frequencies are determined based on the evaluation presented in Section III. The second step consisted in applying the leaky least-mean square multi-channel adaptive filtering (MCAF) algorithm. The reference signals was formed as a subset of ETI components, i.e., magnitude, in-phase, and quadrature, per 1 or 4 EEG channels.

The MCAF algorithm assumes that the clean EEG signal (with no motion artifact impact), denoted with EEG_k, is linearly combined with the signals stemming from motion artifact (m_k). The measured measured signal at each EEG channel k (d_k) can then be expressed as shown in Equation 1.

$$d_k = EEG_k + m_k \tag{1}$$

The MCAF uses subsequent vector observations, where the t-th observation (i.e., at sample time t) can be expressed as shown in Equation 2. Here, $\mathbf{r}[t]$ is the observation of the multi-channel reference signal $\mathbf{r}$, observed at sampling time t. In our case, $\mathbf{r}$ will contain one or more ETI signals that are taken into account within the MCAF algorithm application (see Section III). In this equation, D represents the time lags or the number of filter coefficients used, and T is the matrix transpose operator.

$$\mathbf{I}[t] = [\mathbf{r}[t]^T \mathbf{r}[t-1]^T \mathbf{r}[t-2]^T ... \ \mathbf{r}[t-D]^T]^T \tag{2}$$

$$\mathbf{w}[t+1] = (1 - \mu\alpha) \times \mathbf{w}[t] + \mu \times \epsilon[t]\mathbf{I}[t]/||\mathbf{I}[t]|| \tag{3}$$

$$\epsilon[t] = d[t] - \mathbf{w}^T[t]\mathbf{I}[t] \tag{4}$$

The coefficient values of the AF ($\mathbf{w}[t]$) are updated for each observation time instance t, using an iterative algorithm, as shown in Equation 3 [13]. This algorithm is also known as multiple-input canceler least-mean square AF. In the equation, α is the forgetting factor (such that the expression $b = 1 - \mu\alpha$ is between 0 and 1), μ is the step size of the algorithm (between 0 and 2), and $\epsilon[t]$ is the estimation error. Estimation error is computed as shown in Equation 4. The 'cleaned' EEG signal at the time instant t is than equal to

the estimation error, as we assume that the EEG signal is uncorrelated with the linear combination of reference ETIs.

The parameters of MCAF, namely step size, forgetting factor, and number of coefficients, impact the performance of the AF algorithms. Therefore, we empirically determined their optimal values when using different ETI component combinations as reference signals (as shown in Section III).

D. Evaluation metrics

In the evaluation step we computed the power spectrum and the signal histogram (i.e., probability density function, pdf) of the two 60s **baseline** sections at the start and end of each recording, and compared them to each other and to the motion artifact **contaminated** segments of EEG signals before and after MAR algorithm application. We used two scores that are based on spectral similarities and differences in the pdf (introduced in [11]):

- *Spectral Score (S-Score)*: The mean absolute difference between the power spectra of the segment under test and baseline EEG power spectra, normalized with respect to the baseline EEG power spectra (last 60s). The power spectra in the frequency band between 1 and 40Hz was computed.
- *Distribution Score (D-Score)*: The maximum distance in the empirical cumulative distribution function (ecdf) between the EEG segment under test and baseline EEG.

The lower the value of the scores, the better the performance of the method.

III. RESULTS

A. EEG and ETI

As a first step in designing the proper MAR approach we explored the impact of motion artifacts on EEG and ETI magnitude signals. Figure 2 illustrates the differences in the spectral content of a clean and motion contaminated segments, depicting EEG (top graph), ETI magnitude (middle graph), and the coherence between the two (bottom graph). These figures illustrate the spectra of Cz channel of Participant 1 while he was performing head nodding movement with eyes closed. Similar profiles were observed with other participants, during different movements, and across all 4 channels.

A substantial increase in EEG spectral content below the frequency of 5Hz (delta band brain activity), a medium increase in the range of 5-20Hz (alpha and low beta bands), and a smaller increase of spectra in the higher frequency range can be observed. This demonstrates that the impact of the motion artifact influences a wide range of frequency components of the EEG but to a different extent. The middle graph shows that the ETI frequency components below 25Hz are highly affected by motion artifacts, while this is not the case for higher frequency components. This suggests limited potential of ETI to capture the impact of motion artifacts on the higher frequency components of the EEG (i.e., beta and gamma bands).

Finally, the coherence between the EEG and ETI signal of up to 2Hz is quite high for segments with no artifacts,

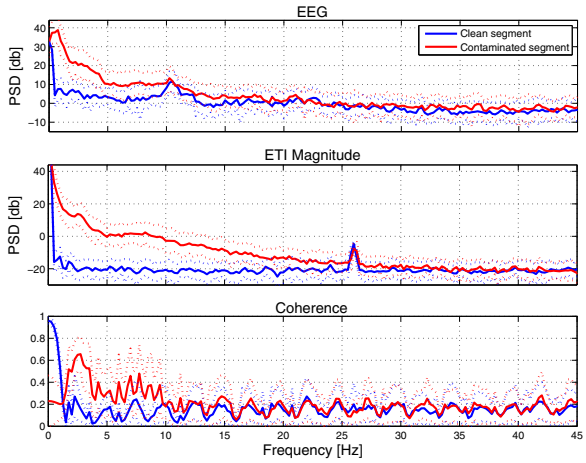

Fig. 2. Spectral content of the EEG signal, ETI magnitude, and coherence between the two. Participant 1 Cz channel data while performing head nodding with eyes closed is shown. Dashed lines represent standard deviation.

and quite low in the rest of the frequency band of interest. However, in the motion artifact segment, the coherence below 2Hz drops substantially, while it increases in the frequency band of up to 15Hz. Therefore, we inferred that the changes of the ETI magnitude in the frequency band of up to few Hz are not correlated to the changes in the EEG due to motion. Also, the absence of the increase of coherence between the clean and motion artifact contaminated EEG signal at the higher frequency band suggests limited usefulness of ETI for MAR in frequencies higher than 15Hz.

B. Combining BPF and AF

To test the impact of band pass filter on the performance of the AF algorithm, we computed S-Scores and D-Scores of the BPF/AF approach for different high and low pass values. The high-pass values used were: 0.25, 0.5, 1, 1.5, and 2Hz; the low-pass values were: 10, 15, 20, 25, and 35Hz. We used only ETI magnitude component of a single channel, coefficient number (D) was 1024, step size (μ) was 0.5, and forgetting factor (α) was 0.1. An illustration of the S-Score and D-Score curves is shown in Figure 3. Although they depict score values for Participant 1 while he was performing different head movements, similar behavior can be observed with the other five participants. As can be seen in the figure, the best performance (i.e., the lowest scores) are achieved with higher values of low and high pass filters.

Furthermore, we compared the scores when using different combinations of ETI components as the reference signal for adaptive filtering. BPF in the 2-35Hz range was employed. The components used are ETI magnitude, in-phase, and quadrature components. The reference consisted either of one of these components or their combination for a single channel and for all 4 channels. Empirical evaluation of the performance was used to select the step size: 0.5 for 1 component, 0.4 for 2 components, 0.3 for 3 components, 0.15 for 4 components, and 0.06 for 8 or 12 components of ETI. The same values for forgetting factor as in the previous evaluation and the coefficient number of 128 (as we low pass filtered the signals) were used.

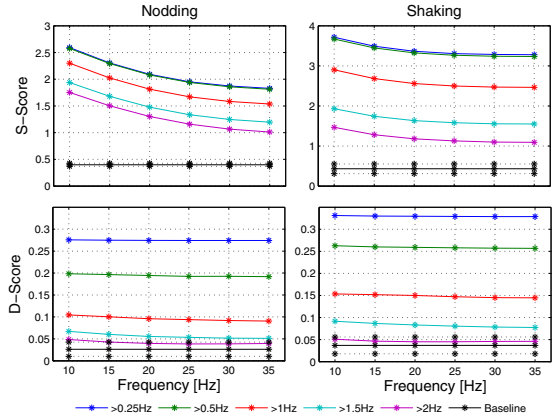

Fig. 3. The influence of band-pass filtering on S-Scores and D-Scores across different sessions for Participant 1, aggregated per channel. The black line shows the baseline score values

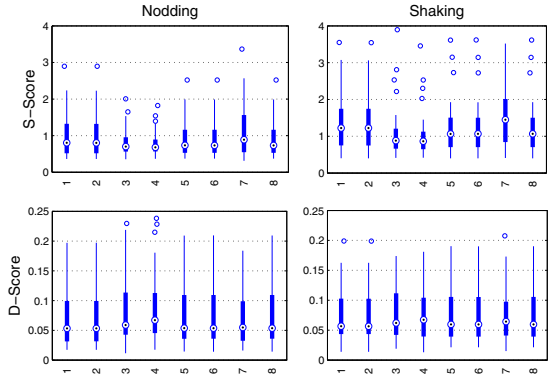

Fig. 4. The values of S-Score and D-Score when different ETI components are used, aggregated over all participants and channels. Identifiers 1 to 4 correspond to single channel ETI components: 1 - magnitude, 2 - in-phase, 3 - in-phase and quadrature, and 4 - all three components. Identifiers 5 to 8 represent the same combinations but across all 4 channels.

The outcome, shown in Figure 4, revealed that combining all ETI components within a single channel into a reference signal for MCAF results in the lowest S-scores, but highest D-Scores. This result does not support our previous finding that combining ETI components per single channels and across all channels improves performance of MAR algorithms [11]. We believe that the difference in the results was due to removal of large motion artifacts in the low frequency range performed using BPF. Using more reference components could to some extent capture a portion of this low-frequency artifacts.

In sum, our BPF/AF method is capable of performing substantial reduction of motion artifacts, as illustrated in Figure 5. However, due to the 2Hz high-pass filtering it also impacts the low frequency EEG content (in the delta band), making low-frequency EEG monitoring difficult. Also, estimating to what degree motion artifact components are still present in the cleaned EEG signal is still an open question. This aspect and the usage of other motion artifact handling methods are some of the topics for further investigation.

IV. CONCLUSIONS

This paper investigated the impact of head motion artifacts on EEG and electrode-tissue impedance (ETI) signals recorded with a wearable, wireless EEG headset with integrated dry electrodes. We have shown that components of the ETI signal (magnitude, in-phase, and quadrature) are not capable of capturing low-frequency (lower than 2Hz) changes in EEG stemming from motion artifacts. We proposed a method that combines the band-pass and adaptive filtering to cope with the limitations of the reference ETI signal. We have shown that this method can achieve substantial reduction of motion artifacts.

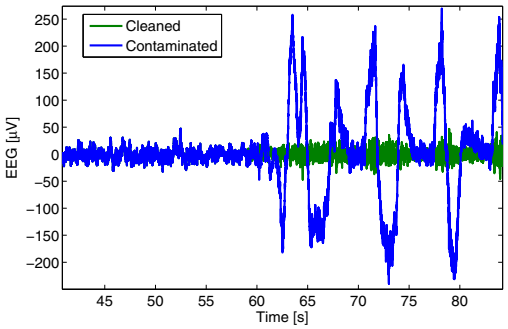

Fig. 5. The result of applying MCAF on a portion of recorded signal.

REFERENCES

[1] Y. M. Chi, T.-P. Jung, and G. Cauwenberghs, "Dry-contact and Non-contact Biopotential Electrodes," *IEEE Reviews in Biomedical Engineering*, vol. 3, no. 1, pp. 106–119, 2010.

[2] J. T. Gwin, K. Gramann, S. Makeig, and D. P. Ferris, "Removal of Movement Artifact From High-Density EEG Recorded During Walking and Running," *Journal of Neurophysiology*, vol. 103, no. 6, pp. 3526–3534, 2010.

[3] K. T. Sweeney, T. E. Ward, and S. F. McLoone, "Artifact Removal in Physiological Signals - Practices and Possibilities," *IEEE Transactions on Information Technology in Biomedicine*, vol. 16, no. 3, pp. 488–500, 2012.

[4] V. Mihajlović, H. Li, B. Grundlehner, J. Penders, and A. C. Schouten, "The Effect of Force and Electrode Material on Electrode-to-Skin impedance," in *BioCAS*, 2012, pp. 57–60.

[5] S. O'Regan and W. Marnane, "Multimodal Detection of Head-Movement Artefacts in EEG," *Journal of Neuroscience Methods*, vol. 218, no. 1, pp. 110–120, 2013.

[6] S. O'Regan, S. Faul, and W. Marnane, "Automatic Detection of EEG Artefacts Arising from Head Movements Using EEG and Gyroscope Signals," *Medical Engineering & Physics*, vol. 35, no. 7, pp. 857–874, 2013.

[7] K. T. Sweeney, D. J. Leamy, T. E. Ward, and S. McLoone, "Intelligent Artifact Classification for Ambulatory Physiological Signals," in *EMBC*, 2010, pp. 6349–6352.

[8] K. T. Sweeney, S. F. McLoone, and T. E. Ward, "The Use of Ensemble Empirical Mode Decomposition with Canonical Correlation Analysis as a Novel Artifact Removal Technique," *IEEE Transactions on Biomedical Engineering*, vol. 60, no. 1, pp. 97–105, 2013.

[9] A.-M. Tautan, V. Mihajlović, Y.-H. Chen, B. Grundlehner, J. Penders, and W. Serdijn, "Signal Quality in Dry Electrode EEG and the Relation to Skin-electrode Contact Impedance Magnitude," in *BIODEVICES*, 2014.

[10] V. Mihajlović, H. Li, B. Grundlehner, J. Penders, and A. C. Schouten, "Investigating the Impact of Force and Movements on Impedance Magnitude and EEG," in *EMBC*, 2013, pp. 1466–1469.

[11] A. Bertrand, V. Mihajlović, B. Grundlehner, C. V. Hoof, and M. Moonen, "Motion Artifact Reduction in EEG Recordings using Multi-Channel Contact Impedance Measurements," in *BioCAS*, 2013.

[12] S. Patki, B. Grundlehner, A. Verwegen, S. Mitra, J. Xu, A. Matsumoto, J. Penders, and R. F. Yazicioglu, "Wireless EEG System with Real Time Impedance Monitoring and Active Electrodes," in *BioCAS*, 2012, pp. 108–111.

[13] S. O. Haykin, Ed., *Adaptive Filter Theory*, 4th ed. Prentice Hall, 2001.